Am J Transl Res 2026;18(7):6132-6150
www.ajtr.org /ISSN:1943-8141/AJTR0173486

Original Article

Resveratrol attenuates LPS-induced oxidative stress and apoptosis in HMC3 microglial cells, partly involving NRF2-related signaling

Yousu Shen[1,2], Mingsheng Zhang[2], Xiaobing Liu[2], Xia Jin[2], Fen Liu[3]

[1]Jiangxi Medical College, Nanchang University, Nanchang 330006, Jiangxi, China; [2]Department of Anesthesiology, The First Affiliated Hospital of Nanchang Medical College, Jiangxi Provincial People's Hospital, Nanchang 330006, Jiangxi, China; [3]Department of Intensive Care Medicine, The First Affiliated Hospital of Nanchang University, Jiangxi Provincial People's Hospital, Nanchang 330006, Jiangxi, China

Received April 21, 2026; Accepted June 8, 2026; Epub July 15, 2026; Published July 30, 2026

Abstract: Postoperative cognitive dysfunction (POCD) is associated with neuroinflammation and oxidative stress, but the underlying mechanisms remain unclear. Resveratrol (RES), a natural polyphenol, has shown neuroprotective potential; however, its effects on microglial injury related to postoperative neuroinflammation have not been fully characterized. In this study, potential shared targets of RES and POCD were first explored using network pharmacology, followed by experimental validation using an LPS-stimulated HMC3 microglial cell model. HMC3 cells were treated with LPS (1000 ng/mL) and RES (50 μM), either with or without the NRF2 inhibitor ML385 (1 μM). Cell viability, proliferation, apoptosis, ROS production, and NRF2-related markers were assessed using CCK-8, EdU staining, flow cytometry, qPCR, Western blotting, and immunofluorescence. Network pharmacology suggested that apoptosis- and NRF2-related antioxidant pathways may be involved in the effects of RES. LPS reduced cell viability and proliferation and increased apoptosis, ROS production, BAX expression, and Caspase-3-related expression. RES partially reversed these changes, increased NRF2, HO-1, and SOD2 expression, and decreased KEAP1 expression under LPS-stimulated conditions. These RES-associated effects were partly weakened by ML385. Overall, RES may attenuate LPS-induced oxidative stress and apoptosis in HMC3 microglial cells, partly involving NRF2-related signaling. This study provides in vitro evidence supporting the potential protective role of RES in microglial injury related to postoperative neuroinflammation.

Keywords: Resveratrol, HMC3, microglia, NRF2, oxidative stress, apoptosis

Introduction

Postoperative cognitive dysfunction (POCD) frequently occurs after surgery and may seriously impair the quality of life of patients. Approximately 10-54% of patients develop POCD within the first few weeks after surgery [1-3]. Factors contributing to POCD include neuroinflammation, oxidative stress, autophagy impairment, synaptic dysfunction, and reduced neurotrophic support. POCD is also associated with various neuropsychiatric conditions, such as dementia, depression, and Alzheimer's disease [4]. However, the pathogenesis of POCD remains incompletely understood, and current findings are not entirely consistent. A key factor in POCD is the systemic inflammatory reaction induced by surgery. Following surgery, circulating inflammatory cytokines, including IL-1, IL-6, and TNF-α, are often elevated. These factors can further induce inflammatory responses in the central nervous system through multiple mechanisms. For example, perioperative TNF-α can increase blood-brain barrier permeability. These changes may exacerbate neuroinflammation and delirium, contributing to POCD [5-7].

As the resident immune cells of the central nervous system (CNS), microglia help maintain brain homeostasis and regulate neuroinflammatory responses [8, 9]. Even in the absence of infection, surgical injury can activate innate immunity. This response leads to increased

https://doi.org/10.62347/XSPN8590

pro-inflammatory cytokines in the hippocampus, which can disrupt neurons involved in learning and memory. Previous studies showed that removing bone marrow-derived macrophages can reduce surgery-induced neuroinflammation and protect memory function [10, 11]. The HMC3 human microglial cell line has been widely used in studies investigating neuroinflammatory mechanisms. Its stable characteristics and robust inflammatory response upon stimulation make it a useful in vitro model [12, 13].

LPS-stimulated microglial models are commonly used to investigate inflammatory and oxidative injury mechanisms relevant to postoperative neuroinflammation and cognitive dysfunction [14, 15]. LPS administration rapidly activates microglia, leading to damage to GABAergic synapses and subsequent long-term cognitive impairment, with significant microglial activation observed in the hippocampus during this period [16, 17]. In microglial cells, LPS stimulation can trigger oxidative stress responses and modulate NRF2-related signaling [18]. ML385, an NRF2 inhibitor, can inhibit the transcriptional activity of NRF2 by directly binding to its DNA-binding domain [19].

Resveratrol is a natural polyphenolic compound found in grapes, peanuts, red wine, and other food sources, known for its various biological activities, including antioxidant, anti-inflammatory, anticancer, neuroprotective, and anti-aging properties [20-22]. Although direct evidence for resveratrol's role in POCD remains limited, substantial evidence indicates that it can modulate oxidative stress and neuroinflammatory responses in several other neurological conditions [23]. Moussa et al. conducted a clinical trial administering resveratrol to patients with mild-to-moderate Alzheimer's disease (AD). They found that resveratrol treatment lowered metalloproteinase-9 (MMP-9) levels in cerebrospinal fluid (CSF) and increased the levels of macrophage-derived chemokine (MDC), interleukin-4 (IL-4), and fibroblast growth factor-2 (FGF-2) [24]. Moreover, resveratrol may reduce inflammation and improve anxiety- and depression-like behaviors caused by maternal separation through the SIRT1/NF-κB pathway [25]. Therefore, investigating whether resveratrol can attenuate microglial injury relevant to postoperative neuroinflammation and exploring the underlying molecular mechanisms represents a meaningful research direction.

In this study, the potential molecular mechanisms of resveratrol (RES) were investigated using network pharmacology. Subsequently, an LPS-induced injury model was established in HMC3 microglial cells to study the protective role of RES. To better understand its mechanism of action, we focused on the NRF2 pathway, which is known to be involved in oxidative stress and apoptosis. Our results provide experimental evidence that RES may attenuate LPS-induced microglial injury associated with oxidative stress and apoptosis.

Materials and methods

Network pharmacology analysis

Identification of targets associated with RES and POCD: RES-related targets were retrieved from the TCMSP database [26]. POCD-related targets were obtained from the GeneCards database by searching the keyword "postoperative cognitive impairment" [27]. This term was selected because it broadly describes postoperative cognitive decline and is conceptually related to postoperative cognitive dysfunction. Then, a filter (relevance score > 0.7) was applied to extract the final set of disease targets.

Screening core targets of RES: The score (MCODE-score) values for each subcluster were analyzed and evaluated using the MCODE plugin of Cytoscape [28]. The subclusters with the highest score were selected. The shared targets of RES and POCD were analyzed with the EcCentricity algorithm in the CytoHubba plugin to identify hub targets.

Protein-protein interaction (PPI) network construction: Possible therapeutic targets for POCD were obtained by identifying the overlapping targets between RES and POCD-related genes. These common genes were entered into the STRING 11.0 database [29], with the species set to *Homo sapiens* and the combined interaction score > 0.9. Unconnected nodes were hidden, and the PPI network was finally shown using Cytoscape 3.9.1.

Gene ontology (GO) enrichment analysis: GO functional enrichment analysis of targets asso-

ciated with RES and POCD was performed using the clusterProfiler package, with the identifier set as "OFFICIAL_GENE_SYMBOL" and the species set as Homo sapiens. The obtained data were used to generate the histogram statistics for CC, MF, and BP. The first twenty data points for CC, MF, and BP are shown on the bars.

KEGG pathway enrichment analysis: The therapeutic targets of RES were converted from 'SYMBOL' to the 'UniProtKB' using the UniProt database (https://www.uniprot.org/) [30]. Next, the KEGG IDs were obtained and the path information of the target was matched using the KEGG Mapper (https://www.genome.jp/kegg/mapper/) [31]. Finally, the color of the relevant genes in the pathway was modified for the subsequent analysis and prediction of the POCD therapeutic pathway.

In vitro assay

Cell culture and treatment: HMC3 human microglial cells (CL-0620; Wuhan Procell Biotechnology Co., Ltd., Wuhan, China) were cultured in EMEM medium (Corning, USA) supplemented with 10% fetal bovine serum (FBS; Gibco, USA) and 1% antibiotics at 37°C in a humidified incubator containing 5% CO_2. Cells were seeded into 6-well plates at 2×10^5 cells per well or into 96-well plates at 5×10^3 cells per well. Resveratrol (RES; 3,4',5-trihydroxy-trans-stilbene; purity ≥ 98.0%; Merck KGaA, Darmstadt, Germany; MFCD00133799) was dissolved in dimethyl sulfoxide (DMSO; HY-Y0320; MedChemExpress, USA) to prepare the stock solution. The final concentration of DMSO was equalized across all groups and did not exceed 0.1%. The control and LPS groups received the same final concentration of DMSO as the vehicle control. Lipopolysaccharide (LPS; L5293; Sigma-Aldrich, USA) was prepared according to the manufacturer's instructions. ML385, an NRF2 inhibitor, was used at a final concentration of 1 μM. The experimental groups were as follows: control, RES alone (50 μM), LPS alone (1,000 ng/mL), LPS + RES, and LPS + RES + ML385. ML385 was used to assess whether NRF2-related signaling was involved in the RES-associated changes under LPS-stimulated conditions. All treatments lasted for 48 h. After treatment, cells were collected for subsequent assays.

CCK-8 assay: To assess cell viability and the cytotoxic profile of various treatments, HMC3 cells were subjected to a CCK-8 assay (GlpBio, USA). Initially, cells were exposed to varying concentrations of LPS (10, 100, or 1,000 ng/mL) across a 24-72 h timeframe, while RES cytotoxicity was screened within 0, 10, 50, 100, or 200 μM over 48 h. Following this optimization, a 48-h treatment with 1,000 ng/mL LPS was established as the experimental baseline. Subsequent evaluations involved four distinct groups: 50 μM RES, 1,000 ng/mL LPS, a combination of LPS and RES, and a triple combination including 1 μM ML385. Viability was quantified by adding 10 μL of CCK-8 reagent 4 h prior to termination, with optical density (OD) recorded at 450 nm.

EdU assay: Cell proliferation was measured using an EdU cell proliferation detection kit (CX003; Shanghai Epizyme Biotechnology Co., Ltd., Shanghai, China). After treatment, the cells were incubated with EdU reagent at 37°C for 2 h. The remaining EdU reagent was removed by washing the cells three times with serum-free medium. The cells were then observed under a fluorescence microscope (OLYMPUS IX73; Olympus, Tokyo, Japan). The percentage of EdU-positive cells was calculated as the number of EdU-positive cells divided by the number of DAPI-positive cells × 100%.

Assessment of reactive oxygen species (ROS): To monitor oxidative stress, HMC3 cells were incubated with the DCFH-DA probe (10 μM; R6033; US Everbright Inc., Suzhou, China) for a 30-minute period at 37°C, following the manufacturer's protocol (R6033, US Everbright). Post-incubation, the removal of non-incorporated dye was achieved through triple washes with serum-deprived medium. ROS-positive populations and their fluorescence mean intensity were subsequently detected by a RaiseCyte 2L6C flow cytometer (Raisecare, China).

Detection of apoptosis: Cell apoptosis was detected using an Annexin V staining kit (Y6026M; US Everbright Inc., Suzhou, China). Briefly, treated cells were collected and incubated with Annexin V dye diluted in binding buffer at a ratio of 1:100 for 15 min at room temperature in the dark. After staining, cells were washed with serum-free medium and analyzed using a RaiseCyte 2L6C flow cytometer (Raisecare, China). The total apoptotic percent-

Table 1. Primer sequences used for real-time quantitative PCR (RT-qPCR)

Gene	Forward primer sequence (5'-3')	Reverse primer sequence (5'-3')
Bcl-2	ATCGCCCTGTGGATGACTGAGT	GCCAGGAGAAATCAAACAGAGGC
BAX	TCAGGATGCGTCCACCAAGAAG	TGTGTCCACGGCGGCAATCATC
Caspase-3	GGAAGCGAATCAATGGACTCTGG	GCATCGACATCTGTACCAGACC
NRF2	CACATCCAGTCAGAAACCAGTGG	GGAATGTCTGCGCCAAAAGCTG
KEAP1	CAACTTCGCTGAGCAGATTGGC	TGATGAGGGTCACCAGTTGGCA
HO-1	CCAGGCAGAGAATGCTGAGTTC	AAGACTGGGCTCTCCTTGTTGC
SOD2	CTGGACAAACCTCAGCCCTAAC	AACCTGAGCCTTGGACACCAAC
GAPDH	AAGGTCATCCCTGAGCTGAA	TGACAAAGTGGTCGTTGAGG

age was calculated from the apoptotic cell populations in the Annexin V/PI flow cytometry plots.

Immunofluorescence staining: After treatment, cells grown on coverslips were fixed with 4% paraformaldehyde for 20 min and permeabilized with 0.1% Triton X-100 (Biosharp, China) for 10 min. Non-specific binding was blocked with 5% bovine serum albumin (BSA; Beyotime, China) for 30 min. Cells were then incubated overnight at 4°C with primary antibodies against NRF2 (AF0639; Affinity Biosciences, China), HO-1 (43966S; Cell Signaling Technology, USA), KEAP1 (8047S; Cell Signaling Technology, USA), or SOD2 (13141T; Cell Signaling Technology, USA). After washing, cells were incubated with a fluorescent secondary antibody (AB150077; Abcam, UK) for 1 h at room temperature. Nuclei were stained with DAPI (Biosharp, China) for 15 min. Images were obtained using a Nikon Eclipse 80i fluorescence microscope (Nikon, Tokyo, Japan). For immunofluorescence quantification, the mean fluorescence intensity of each target protein was measured using ImageJ software and normalized to the control group.

Real-time quantitative PCR (RT-qPCR): Total RNA was extracted from HMC3 cells using TRIzol LS reagent (Invitrogen, USA). Reverse transcription was performed using 1 μg of total RNA and the SuperScript VILO cDNA synthesis kit (Invitrogen, USA). qPCR was conducted using SYBR Green Realtime PCR Super Mix (Mei5 Bioservices, China) in a 20 μL reaction system. GAPDH was used as the internal reference gene. Relative mRNA expression was calculated using the $2^{-\Delta\Delta Ct}$ method. All reactions were performed in duplicate, and primer sequences are listed in **Table 1**.

Western blot: Total protein was extracted from HMC3 cells using RIPA lysis buffer supplemented with protease and phosphatase inhibitors. Protein concentration was measured using a BCA protein assay kit. Equal amounts of protein were separated by SDS-PAGE and transferred onto PVDF membranes. After blocking with 5% non-fat milk, the membranes were incubated overnight at 4°C with primary antibodies against NRF2 (AF0639; Affinity Biosciences, China), phosphorylated NRF2 (ET1608-28; HUABIO, China), HO-1 (43966S; Cell Signaling Technology, USA), KEAP1 (8047S; Cell Signaling Technology, USA), SOD2 (13141T; Cell Signaling Technology, USA), Bcl-2 (3498T; Cell Signaling Technology, USA), BAX (41162S; Cell Signaling Technology, USA), pro-Caspase-3 (9668T; Cell Signaling Technology, USA), or GAPDH (TA802519; OriGene, USA). After washing, the membranes were incubated with HRP-conjugated secondary antibodies for 1 h at room temperature. Protein bands were visualized using an ECL detection system.

Statistical analysis

All quantitative results are expressed as the mean ± standard deviation (SD) derived from a minimum of three independent biological replicates. Statistical significance between groups was evaluated using a one-way analysis of variance (ANOVA) coupled with Tukey's post hoc test for multiple comparisons. A p value < 0.05 was deemed statistically significant. All statistical analyses and figure generation were executed using GraphPad Prism 10.0 software.

Results

Network pharmacology analysis

We utilized network pharmacology analysis to explore the possible molecular mechanisms of RES in pathways related to POCD. The keyword "postoperative cognitive impairment" was en-

tered into the GeneCards database to identify POCD-related targets. After screening GeneCards with a relevance score > 0.7 and removing duplicate records, 2,243 target genes were retained. In addition, 130 target genes related to RES were collected from the TCMSP database. Venn analysis was then performed with the R package Venn, which identified 88 overlapping genes (**Figure 1A**).

These overlapping genes were analyzed in the STRING 11.0 database, specifying Homo sapiens as the selected species and a combined score greater than 0.9. Free targets were hidden, and PPI model was constructed. The final network consists of 81 nodes and 467 edges, where the number of between two nodes is indicative of their interaction strength (**Figure 1B**). The tsv files in the PPI model were imported into the Cytoscape 3.9.1 software for cluster analysis using the MCODE algorithm. The sub-cluster with the largest MCODE score (MCODE Score = 14.778) was selected. From this sub-cluster, the top 10 key hub genes (STAT3, IL6, NFE2L2, CCND1, BCL2L1, CASP3, FOXO1, BCL2, NFKBIA, IL10) were identified using the EcCentricity algorithm and are shown in **Figure 1C**. Among the identified hub genes, NFE2L2 (also known as NRF2) was closely connected with other key nodes in the network. Given that RES is known to enhance the activity of antioxidant enzymes, such as superoxide dismutase (SOD) and catalase (CAT), potentially by activating the NRF2 signaling pathway [32]. Furthermore, the NRF2/HO-1 pathway and the STAT3 pathway are known to regulate each other. Suppression of NRF2/HO-1 signaling may be accompanied by activation of the JAK2/STAT3 cascade, whereas inhibition of JAK2/STAT3 may enhance NRF2/HO-1 signaling [33, 34]. NRF2 activation also upregulates NQO1 and HO-1 expression, which can reduce IL-6 expression induced by ROS [35]. These intricate connections suggest that NFE2L2 may play a central role in the therapeutic effects of RES and warrants further investigation.

We performed KEGG pathway enrichment analysis to explore which signaling pathways may be involved in the effects of RES on POCD. A total of 238 pathways were significantly enriched (adjusted $P < 0.05$), and the top 20 pathways are shown in **Figure 1D**. Several apoptosis-related pathways were strongly enriched, including “Apoptosis”, “Apoptosis - multiple species”, and the “p53 signaling pathway”. The FoxO signaling pathway was also enriched and is known to regulate oxidative stress responses by promoting the expression of antioxidant genes, such as SOD2 and peroxiredoxins, in different cell compartments [36]. Combined with the PPI and KEGG results, four hub genes were mapped to the apoptosis pathway: BCL2, CASP3, BCL2L1, and NFKBIA.

GO enrichment analysis was then performed to further characterize the biological functions of the shared targets. The top GO terms for biological process (BP), cellular component (CC), and molecular function (MF) are shown in **Figure 1E**. In the BP category, many terms were related to apoptosis, including regulation of apoptotic signaling, intrinsic apoptotic signaling, and negative regulation of apoptosis. Oxidative stress-related terms and the term “response to lipopolysaccharide” were also enriched. In the CC category, the targets were enriched in cellular locations related to these processes, including the mitochondrial outer membrane, membrane raft/caveola, protein kinase complex, and cyclin-dependent protein kinase complex. In the MF category, oxidative stress-related functions, including antioxidant activity, heme binding, and tetrapyrrole binding, and apoptosis-related functions, including death domain binding and ubiquitin protein ligase binding, were enriched. Overall, these enrichment results suggest that RES may be involved in both oxidative stress control and apoptosis regulation in POCD-related pathways.

Network pharmacology analysis suggested that apoptosis-related signaling is a key pathway associated with the effects of RES. Furthermore, NRF2 (NFE2L2) exhibited strong connections with other hub genes, and previous studies have documented a direct regulatory role of RES on NRF2 in other diseases. This highlights NRF2’s potential as a therapeutic target for RES. Therefore, NRF2-related antioxidant signaling and apoptosis-related pathways were selected for subsequent experimental validation [37-39].

RES partially restored the decrease in HMC3 cell viability induced by LPS

Cell viability decreased in a concentration-dependent manner following RES treatment, with clear reductions at 100 and 200 μM

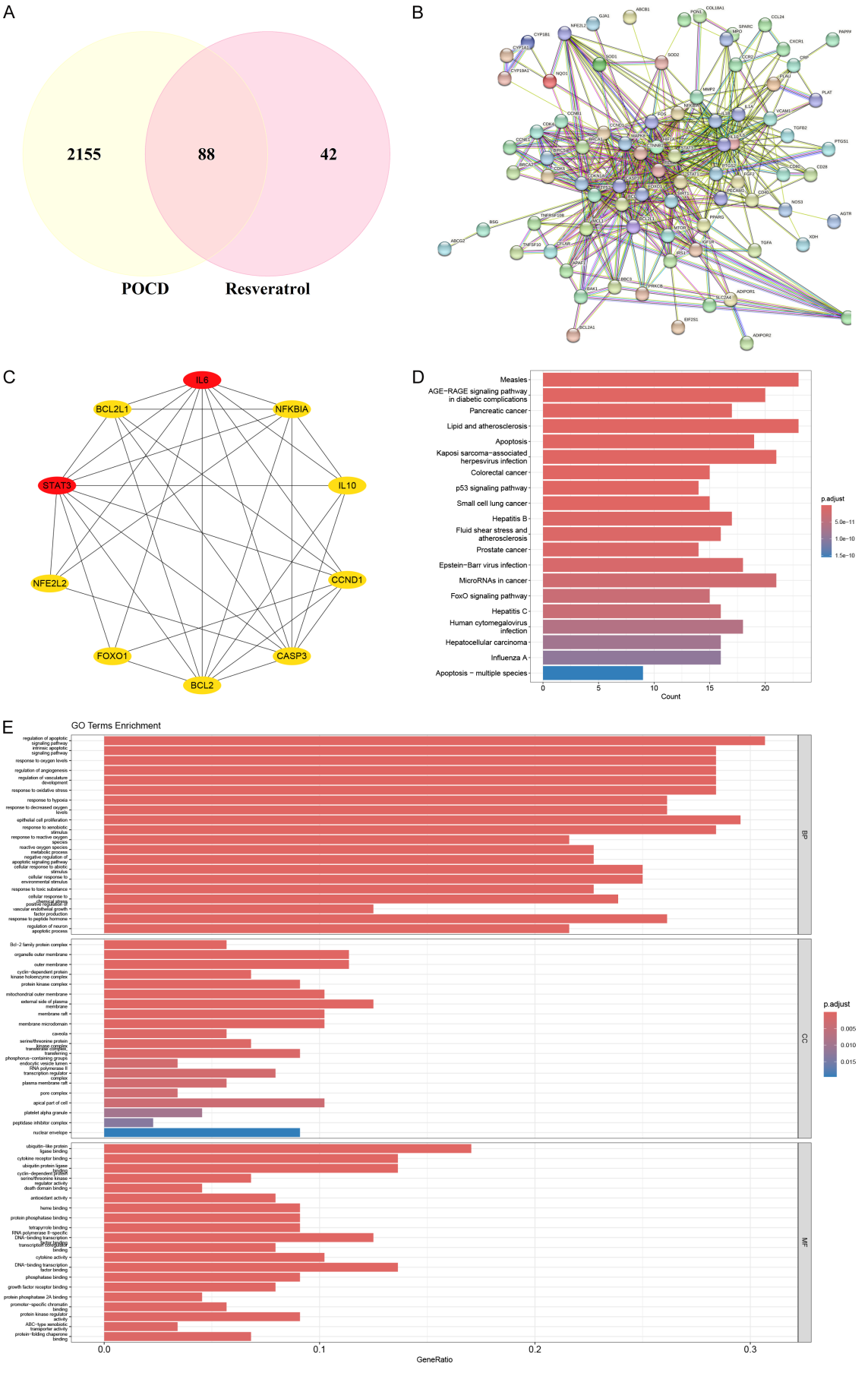
A
2155
88
42
POCD
Resveratrol
B
C
IL6
BCL2L1
NFKBIA
STAT3
IL10
NFE2L2
CCND1
FOXO1
CASP3
BCL2
D
Measles
AGE−RAGE signaling pathway in diabetic complications
Pancreatic cancer
Lipid and atherosclerosis
Apoptosis
Kaposi sarcoma−associated herpesvirus infection
Colorectal cancer
p53 signaling pathway
Small cell lung cancer
Hepatitis B
Fluid shear stress and atherosclerosis
Prostate cancer
Epstein−Barr virus infection
MicroRNAs in cancer
FoxO signaling pathway
Hepatitis C
Human cytomegalovirus infection
Hepatocellular carcinoma
Influenza A
Apoptosis − multiple species
0
5
10
15
20
Count
p.adjust
5.0e−11
1.0e−10
1.5e−10
E
GO Terms Enrichment
BP
CC
MF
p.adjust
0.005
0.010
0.015
0.0
0.1
0.2
0.3
GeneRatio

Figure 1. Network pharmacology analysis of potential shared targets of RES and POCD. Targets of RES and POCD were obtained from the TCMSP and GeneCards databases, respectively. Overlapping targets were used to construct the PPI network. GO and KEGG enrichment analyses were then performed to explore the potential biological processes and pathways associated with the shared targets. A. Venn diagram illustrating the common targets between RES and POCD. B. PPI network depicting the interactions among the potential targets of RES and POCD. C. Hub gene analysis showing the key genes with central roles in the network. D. KEGG pathway analysis revealing the major biological pathways associated with the common targets of RES and POCD. E. GO analysis highlighting the enrichment of these targets in biological processes, molecular functions, and cellular components.

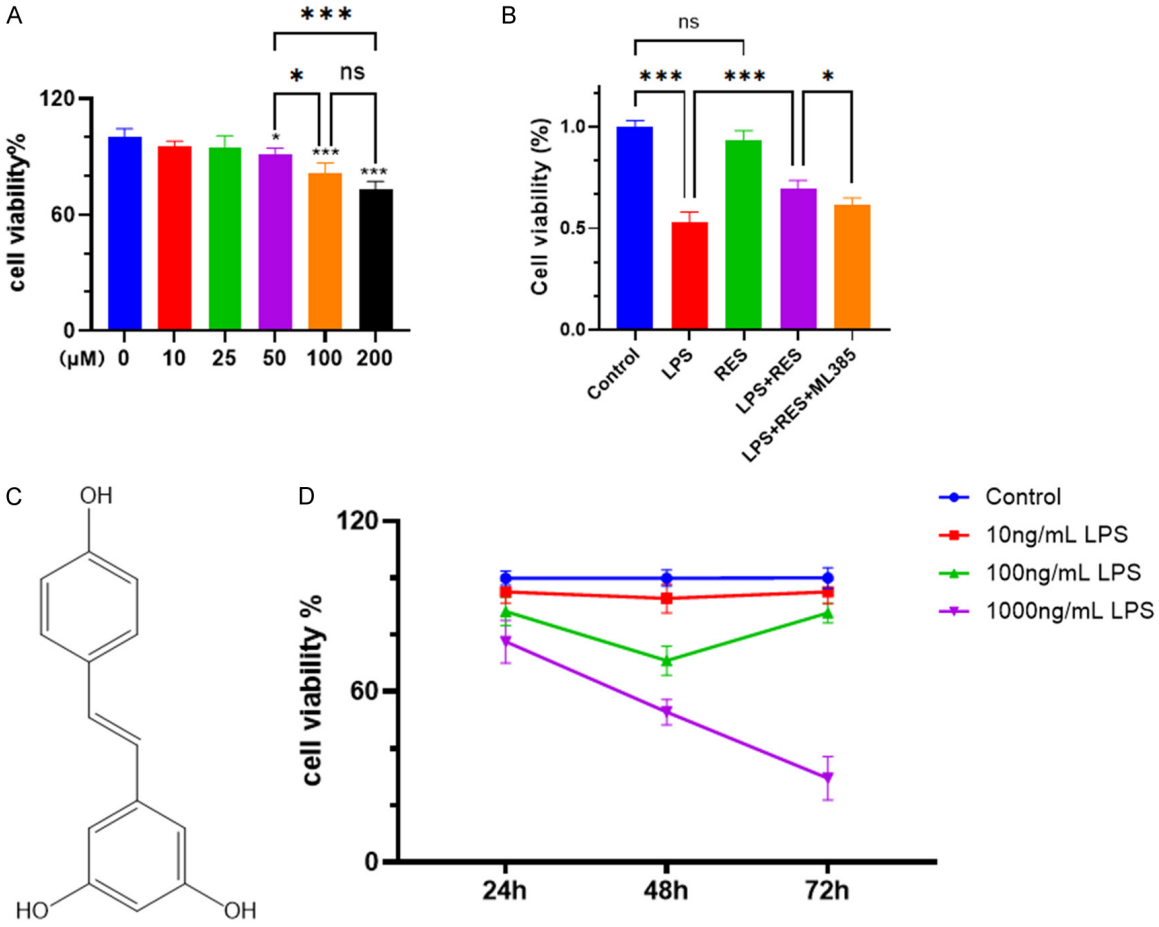

Figure 2. Effects of RES and LPS on HMC3 cell viability. A. HMC3 cells were treated with different concentrations of resveratrol (RES; 0, 10, 25, 50, 100, and 200 μM) for 48 h, and cell viability was measured using the Cell Counting Kit-8 (CCK-8) assay. B. Cell viability in different treatment groups, including control, lipopolysaccharide (LPS), RES, LPS + RES, and LPS + RES + ML385. C. Chemical structure of RES. D. HMC3 cells were treated with different concentrations of LPS (10, 100, and 1000 ng/mL) for 24, 48, and 72 h, and cell viability was measured by CCK-8 assay. Data are presented as the mean ± SD from at least three independent experiments. ns, not significant; *P < 0.05, **P < 0.01, ***P < 0.001.

(**Figure 2A**). Therefore, 50 μM RES was selected for subsequent experiments. In the LPS injury model, RES alone did not significantly affect cell viability compared with the control group. LPS markedly reduced HMC3 cell viability, while RES partially restored this reduction. Compared with the LPS + RES group, the LPS + RES + ML385 group showed lower cell viability, suggesting that ML385 attenuated the RES-associated protective effect under LPS-stimulated conditions (**Figure 2B**). The chemical structure of RES is shown in **Figure 2C**. LPS concentration screening showed that 1,000 ng/mL LPS caused the most obvious reduction in cell viability at 48 and 72 h (**Figure 2D**). Based on these results, 1,000 ng/mL LPS and 50 μM RES for 48 h were selected for subsequent experiments.

RES partially reversed LPS-induced proliferation inhibition in HMC3 cells

Cell proliferation was evaluated using EdU staining. Compared with the control group, LPS treatment reduced the number of EdU-positive HMC3 cells. RES treatment partly increased EdU-positive cells under LPS-stimulated conditions. Quantitative analysis showed that the percentage of EdU-positive cells was lower in the LPS group than in the control group, while it was higher in the LPS + RES group than in the LPS group. Compared with the LPS + RES group, the LPS + RES + ML385 group showed a lower percentage of EdU-positive cells, suggesting that ML385 reduced the RES-associated improvement in cell proliferation under LPS-stimulated conditions (**Figure 3**).

RES attenuated LPS-induced apoptosis in HMC3 cells

Apoptosis in HMC3 cells was measured by Annexin V staining. The total apoptotic percentage was calculated from the apoptotic cell populations shown in the Annexin V/PI flow cytometry plots. Compared with the control group, LPS increased the percentage of apoptotic cells. RES reduced LPS-induced apoptosis. Compared with the LPS + RES group, the LPS + RES + ML385 group showed a higher apoptotic percentage, suggesting that ML385 partly reduced the RES-associated anti-apoptotic effect under LPS-stimulated conditions (**Figure 4**).

RES inhibited the LPS-induced ROS production in HMC3 cells

We next examined ROS production in LPS-treated HMC3 cells. LPS markedly increased intracellular ROS compared with the control group. RES treatment reduced ROS levels in LPS-stimulated cells. Compared with the LPS + RES group, the LPS + RES + ML385 group showed higher ROS levels, suggesting that ML385 partly reduced the RES-associated suppression of ROS production under LPS-stimulated conditions (**Figure 5**).

RES attenuated LPS-induced changes in apoptosis-related markers in HMC3 cells

Representative Western blot bands are shown in **Figure 6A**. The LPS group showed higher expression of BAX and pro-Caspase-3 proteins than the control group, while Bcl-2 protein expression remained largely unchanged. RES treatment attenuated the LPS-induced increases in BAX and pro-Caspase-3. Compared with the LPS + RES group, the LPS + RES + ML385 group showed higher BAX protein expression, while pro-Caspase-3 protein expression showed a slight but non-significant increase (**Figure 6B** and **6D**). There was no significant difference in Bcl-2 protein levels among the groups (**Figure 6C**). Similar patterns were observed at the mRNA level. LPS upregulated BAX and Caspase-3 mRNA expression, whereas RES reduced these changes. Compared with the LPS + RES group, the LPS + RES + ML385 group showed higher BAX and Caspase-3 mRNA expression (**Figure 6E** and **6G**), while Bcl-2 mRNA expression remained unchanged (**Figure 6F**). Together, these data suggest that RES may mitigate LPS-induced apoptotic responses in HMC3 cells.

RES was associated with enhanced NRF2-related antioxidant signaling in LPS-treated HMC3 cells

Immunofluorescence staining and quantitative analysis were used to evaluate HO-1, KEAP1, NRF2, and SOD2 expression. Compared with the control group, LPS increased the fluorescence intensity of HO-1, NRF2, and SOD2, while KEAP1 fluorescence intensity was reduced. Compared with the LPS group, the LPS + RES group showed higher HO-1, NRF2, and SOD2 fluorescence intensity and lower KEAP1 fluorescence intensity. After ML385 was added to the LPS + RES treatment, HO-1, NRF2, and SOD2 fluorescence intensity decreased, while KEAP1 fluorescence intensity partly increased compared with the LPS + RES group (**Figure 7A-D**). These results suggest that RES may enhance NRF2-related antioxidant responses under LPS-stimulated conditions, and that this effect may be partly weakened by ML385.

Western blot analysis showed similar trends. Compared with the control group, LPS increased the protein levels of HO-1, p-NRF2, NRF2, and SOD2, while KEAP1 protein expression was decreased. Compared with the LPS group, RES treatment further increased HO-1, p-NRF2, NRF2, and SOD2 protein levels and further reduced KEAP1 expression. In the LPS + RES +

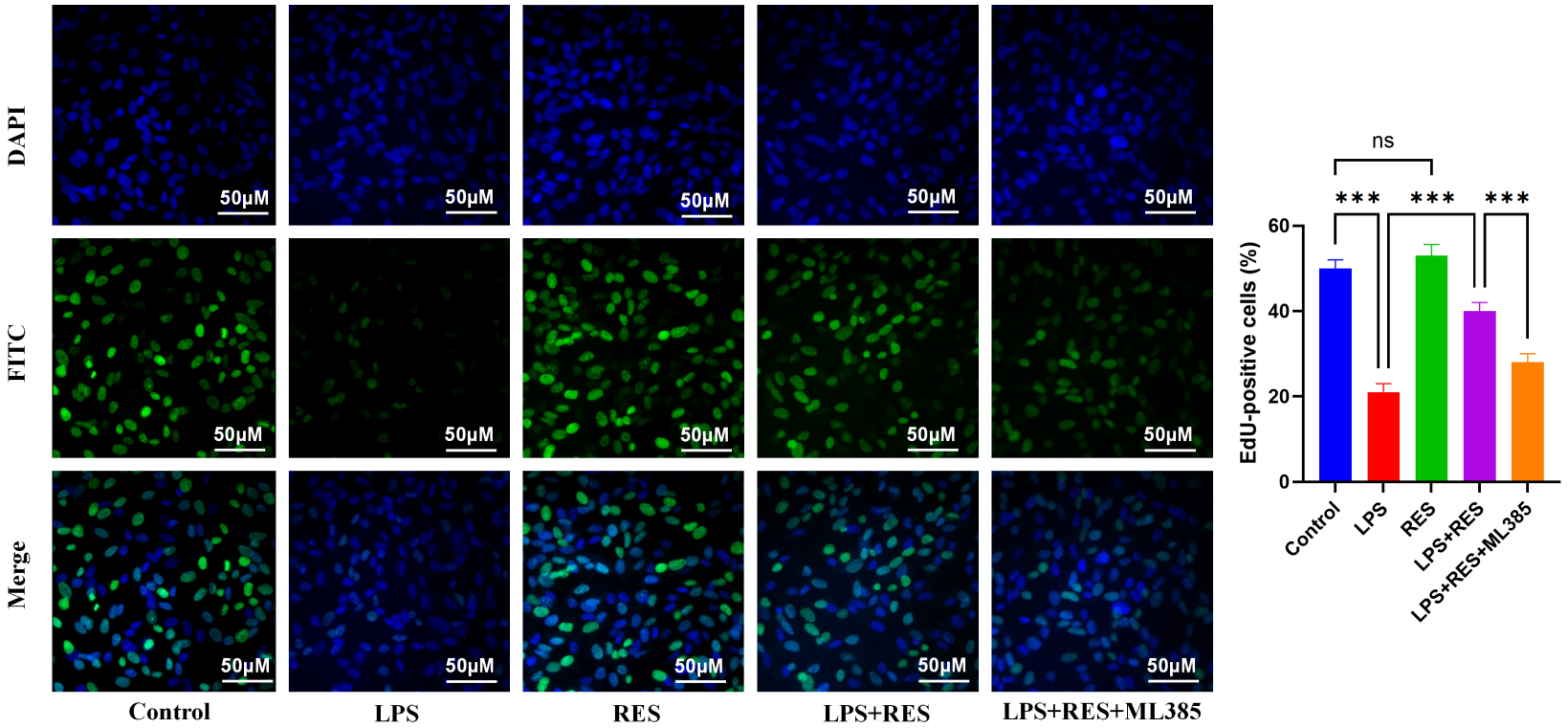

Figure 3. EdU assay showing the effects of RES on LPS-induced proliferation inhibition in HMC3 cells. HMC3 cells were treated for 48 h in the following groups: control, RES (50 μM), LPS (1000 ng/mL), LPS + RES, and LPS + RES + ML385. DAPI staining (blue) shows cell nuclei, and FITC staining (green) shows EdU-positive proliferating cells. Merged images show the overlap of DAPI and FITC staining. The bar graph shows the percentage of EdU-positive cells among total DAPI-positive cells. Data are presented as the mean ± SD from three independent experiments. ns, not significant; ***P < 0.001. Scale bar: 50 μm.

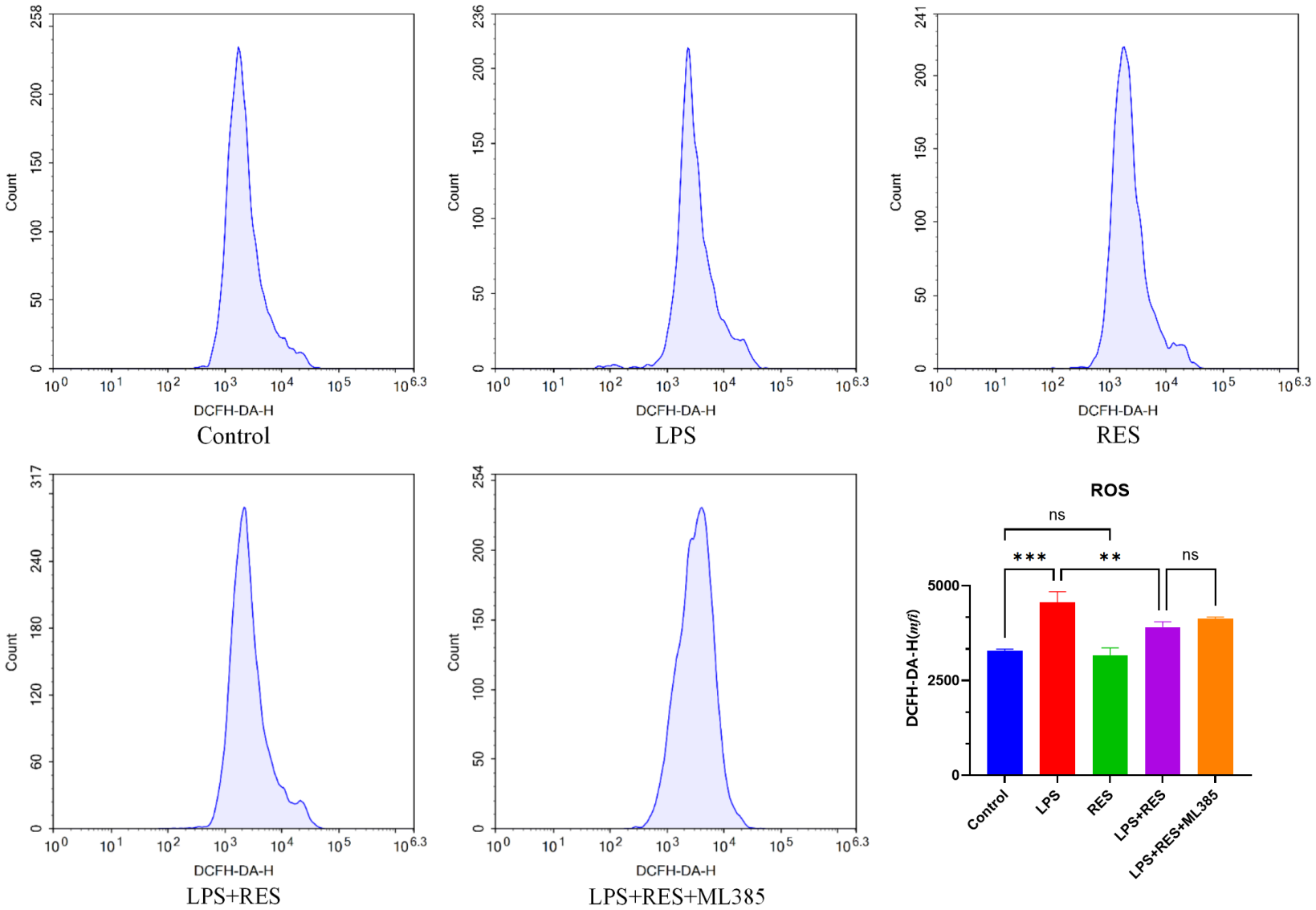

Figure 4. RES attenuated LPS-induced apoptosis in HMC3 cells. HMC3 cells were treated for 48 h in the following groups: control, resveratrol (RES; 50 μM), lipopolysaccharide (LPS; 1000 ng/mL), LPS + RES, and LPS + RES + ML385. Cell apoptosis was detected by Annexin V-fluorescein isothiocyanate (FITC)/propidium iodide (PI) flow cytometry. The X-axis represents Annexin V-FITC staining, and the Y-axis represents PI staining. The bar graph shows the total apoptotic percentage calculated from the apoptotic cell populations in the flow cytometry plots. Data are presented as the mean ± SD from at least three independent experiments. ns, not significant; **P < 0.01, ***P < 0.001.

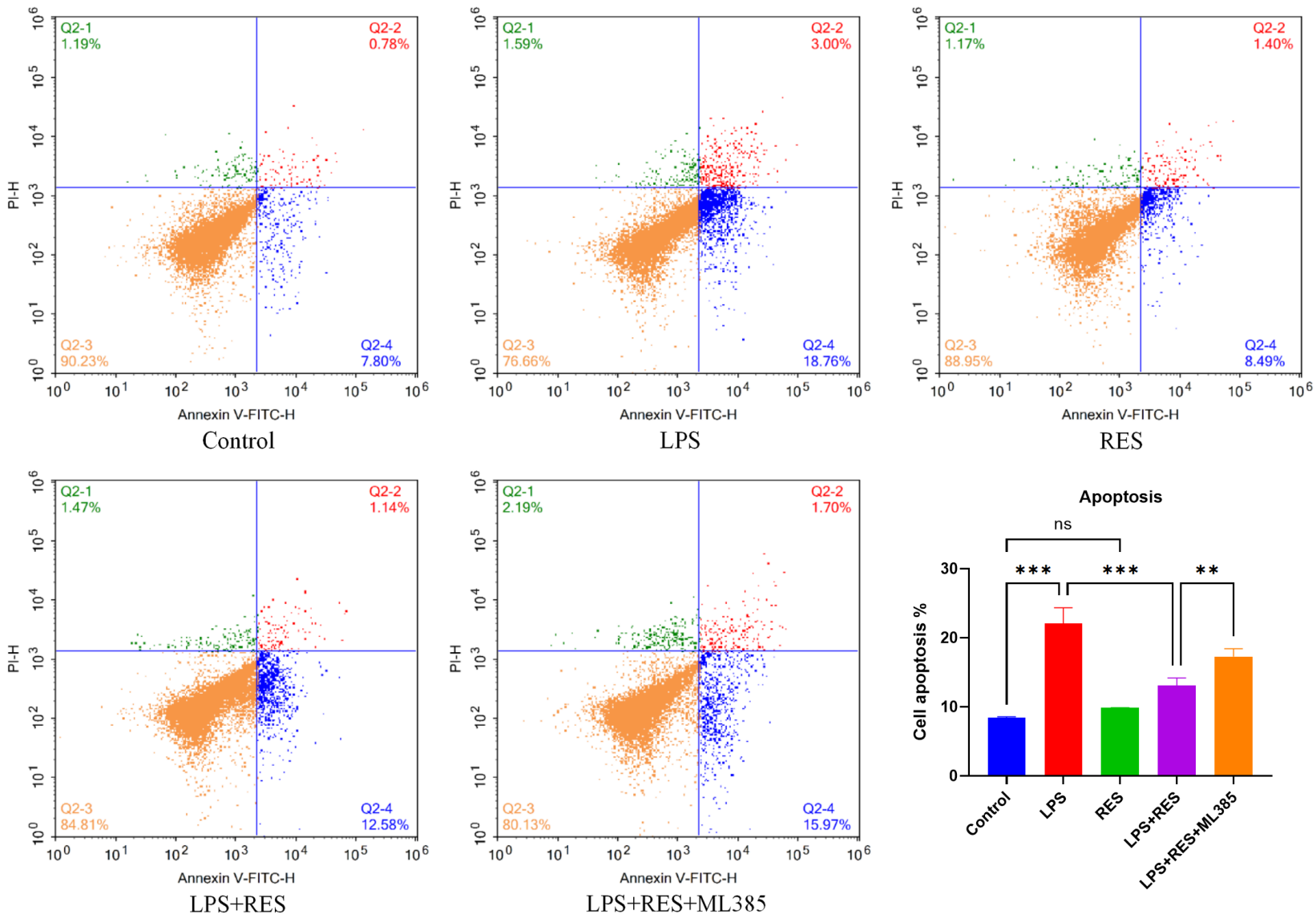

Figure 5. RES reduced LPS-induced ROS production in HMC3 cells. HMC3 cells were treated for 48 h in the following groups: control, resveratrol (RES; 50 μM), lipopolysaccharide (LPS; 1000 ng/mL), LPS + RES, and LPS + RES + ML385. Intracellular reactive oxygen species (ROS) levels were detected using the 2',7'-dichlorodihydrofluorescein diacetate (DCFH-DA) probe and analyzed by flow cytometry. Representative flow cytometry histograms are shown for each group. The bar graph shows the mean fluorescence intensity of DCFH-DA. Data are presented as the mean ± SD from at least three independent experiments. ns, not significant; **P < 0.01, ***P < 0.001.

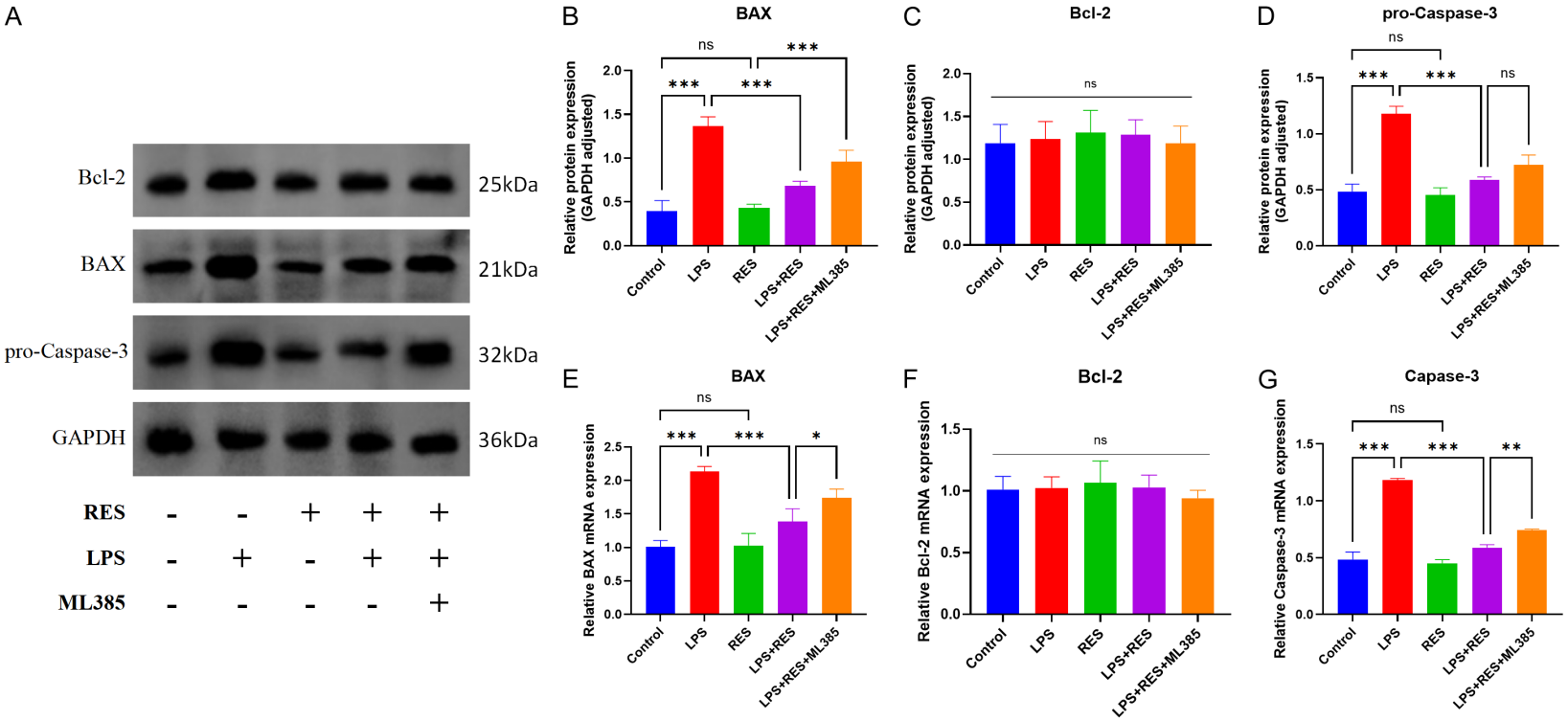

Figure 6. RES attenuated LPS-induced changes in apoptosis-related markers in HMC3 cells. HMC3 cells were treated for 48 h in the following groups: control, resveratrol (RES; 50 μM), lipopolysaccharide (LPS; 1,000 ng/mL), LPS + RES, and LPS + RES + ML385. A. Representative Western blot bands showing the protein expression of Bcl-2, BAX, pro-Caspase-3, and GAPDH. GAPDH was used as the loading control. The analyzed Caspase-3 band corresponded to pro-Caspase-3, and cleaved Caspase-3 fragments were not quantified in this study. B-D. Quantification of BAX, Bcl-2, and pro-Caspase-3 protein expression normalized to GAPDH. E-G. Quantification of relative mRNA expression levels of BAX, Bcl-2, and Caspase-3, with GAPDH used as the internal reference. Data are presented as the mean ± SD from at least three independent experiments. ns, not significant; *P < 0.05, **P < 0.01, ***P < 0.001.

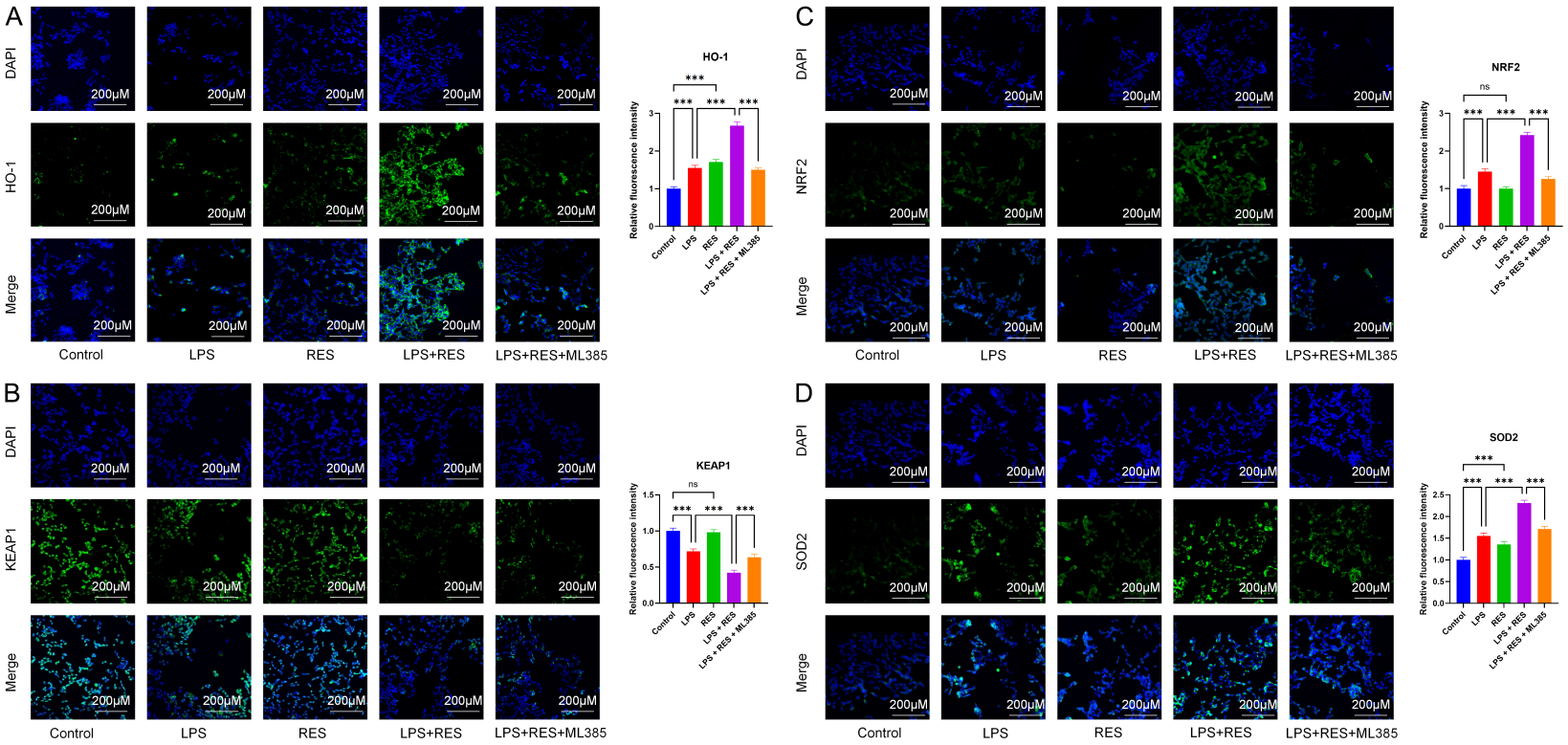

Figure 7. Immunofluorescence analysis of NRF2-related antioxidant markers in HMC3 cells. HMC3 cells were treated with RES, LPS, LPS + RES, or LPS + RES + ML385 for 48 h. Nuclei were stained with DAPI, and target proteins were detected by green fluorescence. A. HO-1. B. KEAP1. C. NRF2. D. SOD2. Bar graphs show the relative fluorescence intensity of each marker. Data are presented as the mean ± SD from at least three independent experiments. ns, not significant; ***P < 0.001. Scale bar: 200 μm.

ML385 group, HO-1, p-NRF2, NRF2, and SOD2 protein levels were lower than those in the LPS + RES group, whereas KEAP1 expression was higher (**Figure 8A-F**). qPCR analysis showed a consistent expression pattern at the mRNA level. RES increased HO-1, NRF2, and SOD2 mRNA expression and decreased KEAP1 mRNA expression under LPS-stimulated conditions, whereas ML385 partly reduced these RES-associated transcriptional changes (**Figure 8G-J**). Together, these results suggest that RES may strengthen NRF2-related antioxidant signaling in LPS-treated HMC3 cells, accompanied by KEAP1 downregulation and increased HO-1 and SOD2 expression.

Discussion

POCD predominantly affects older adults after surgery and is marked by a notable decline in cognitive functions, such as coordination, attention, memory, orientation, executive function, and verbal fluency [40]. At hospital discharge, POCD is reported in about 30% of younger patients and 40% of older patients. After cardiovascular surgery, the incidence can reach approximately 40% within the first week and may still be about 17% at three months [41]. The mechanisms underlying POCD remain incompletely understood, but current evidence implicates central inflammation, neuronal apoptosis, and impaired synaptic plasticity [42, 43]. LPS-stimulated microglial models can be used to investigate cellular mechanisms relevant to postoperative neuroinflammation and oxidative injury [14, 44].

POCD is linked to inflammatory activation of hippocampal microglia. Xiaomei et al. showed that inhibiting colony-stimulating factor 1 receptor (CSF1R) effectively reduces microglia in the central nervous system, protecting against POCD. This effect can lead to reduced levels of inflammatory factors and decreased recruitment of $CCR2^{+}$ leukocytes in the hippocampus [45]. As a transcription factor, NRF2 is important for the regulation of antioxidant genes and anti-inflammatory activity. NRF2 and its main inhibitor, Keap1, work together to maintain cellular redox homeostasis, influence inflammation, and regulate HO-1 expression [46]. RES exhibits a broad range of beneficial pharmacological activities. It can attenuate STZ-induced learning and memory deficits and normalize the abnormal expression of Aβ1-42, Tau, BDNF, and PSD95 [47]. Additionally, as ischemia is a potential cause of POCD, RES administered before injury may protect against focal cerebral ischemia by decreasing BF cell loss and ameliorating cholinergic memory deficits and hippocampal synaptic damage. Therefore, RES represents a promising candidate for further investigation in POCD-related neuroinflammatory injury [48, 49].

In this study, network pharmacology analysis suggested that apoptosis-related pathways and NRF2-associated antioxidant signaling may be involved in the potential effects of RES. Although several hub genes, including STAT3, IL6, NFE2L2, BCL2, and CASP3, were identified by network pharmacology, the present study focused on the NRF2-related oxidative stress and apoptosis axis for several reasons. First, NFE2L2/NRF2 was one of the hub genes in the PPI network and was closely connected with apoptosis- and inflammation-related nodes. Second, GO and KEGG analyses indicated enrichment of oxidative stress- and apoptosis-related biological processes, which were consistent with the main injury phenotype observed in LPS-stimulated HMC3 cells, including ROS accumulation and increased apoptosis. Third, RES has been widely reported to regulate cellular antioxidant responses through NRF2-related signaling pathway, making this pathway biologically plausible for experimental validation. In contrast, although STAT3 and IL6 are also important inflammatory nodes, inflammatory cytokine release and STAT3 phosphorylation were not directly measured in the present study. Therefore, we did not further interpret the STAT3/IL6 axis mechanistically. Future studies should examine whether inflammatory pathways such as IL-6/STAT3 interact with NRF2-related antioxidant signaling in RES-mediated protection against LPS-induced microglial injury.

In vitro experiments showed that LPS induced oxidative stress and apoptosis-related changes in HMC3 cells, as reflected by increased ROS levels and higher expression of BAX and pro-Caspase-3. RES treatment reduced ROS accumulation and apoptosis-related marker expression and improved cell viability under LPS-stimulated conditions. These changes were accompanied by increased NRF2, p-NRF2, HO-1,

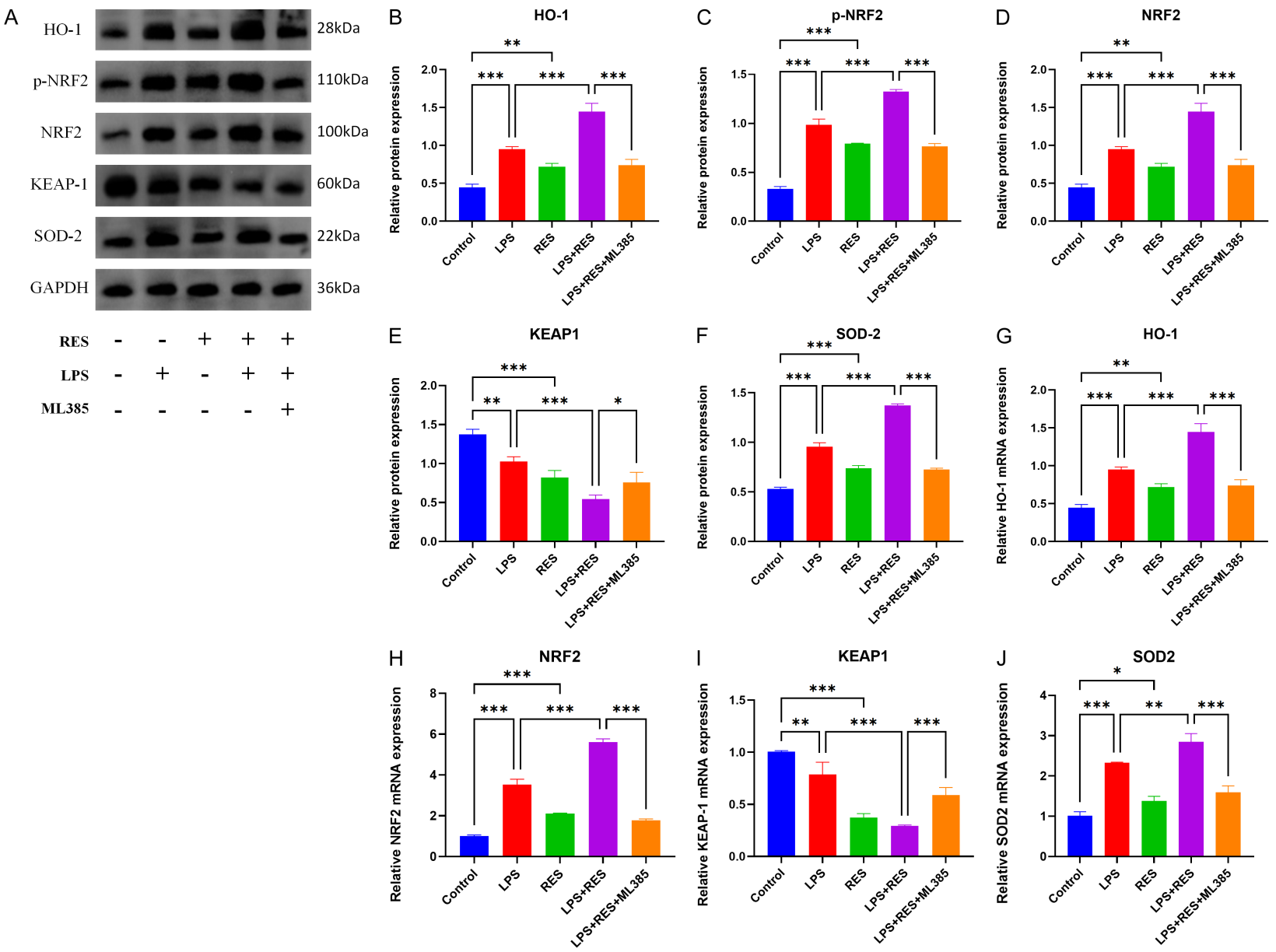
A
HO-1
p-NRF2
NRF2
KEAP-1
SOD-2
GAPDH
28kDa
110kDa
100kDa
60kDa
22kDa
36kDa
RES - - + + +
LPS - + - + +
ML385 - - - - +
B HO-1
C p-NRF2
D NRF2
E KEAP1
F SOD-2
G HO-1
H NRF2
I KEAP1
J SOD2
Relative protein expression
Relative HO-1 mRNA expression
Relative NRF2 mRNA expression
Relative KEAP-1 mRNA expression
Relative SOD2 mRNA expression
Control
LPS
RES
LPS+RES
LPS+RES+ML385

Figure 8. RES enhanced NRF2-related antioxidant signaling in HMC3 cells. HMC3 cells were treated with RES, LPS, LPS + RES, or LPS + RES + ML385 for 48 h. A. Representative Western blot bands of HO-1, p-NRF2, NRF2, KEAP1, SOD2, and GAPDH. B-F. Quantification of protein expression normalized to GAPDH. G-J. Relative mRNA expression levels of HO-1, NRF2, KEAP1, and SOD2. Data are presented as the mean ± SD from at least three independent experiments. *P < 0.05, **P < 0.01, ***P < 0.001.

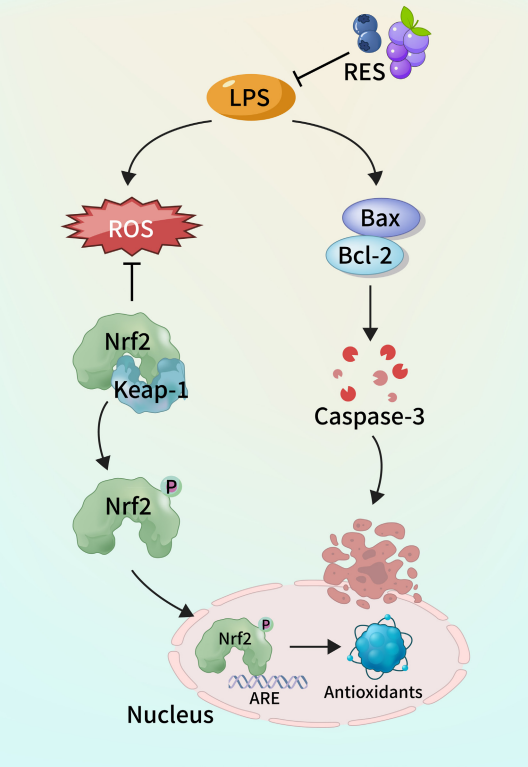

Figure 9. Schematic illustration of the proposed protective effects of RES in LPS-induced HMC3 cell injury. RES may attenuate oxidative stress and apoptosis in LPS-stimulated HMC3 cells, partly involving NRF2-related signaling.

and SOD2 expression and decreased KEAP1 expression. KEAP1 is a key negative regulator of NRF2. Under basal conditions, KEAP1 promotes NRF2 ubiquitination and degradation, thereby limiting NRF2-dependent transcription. When KEAP1 expression or activity is reduced, NRF2 may become more stable and more readily activate downstream antioxidant genes, including HO-1 and SOD2. Therefore, the decrease in KEAP1 observed after RES treatment may help explain the increased NRF2-related signal and the upregulation of HO-1 and SOD2. Compared with the LPS + RES group, the LPS + RES + ML385 group showed partial reduction of these RES-associated antioxidant and anti-apoptotic changes. These findings suggest that NRF2-related signaling, together with a KEAP1-associated regulatory pattern, may be involved in the protective effects of RES in LPS-stimulated HMC3 cells (**Figure 9**).

Several limitations of this work should be noted. First, this study was based on a single LPS-stimulated HMC3 cell model, which cannot fully reproduce the biological features of primary microglia or the complex pathological process of POCD in vivo. Therefore, the protective effects of RES need further validation in primary microglia, animal models, clinical samples, and surgery- or anesthesia-induced POCD models. Second, an ML385-alone group was not included, and ML385, as a pharmacological NRF2 inhibitor, may have concentration- or cell context-dependent effects. Future studies should include an ML385-alone group and use NRF2 knockdown, overexpression, or rescue experiments to confirm the specific role of NRF2. Third, the network pharmacology analysis used “postoperative cognitive impairment” as the GeneCards search term. Although this term is conceptually related to postoperative cognitive dysfunction, different search terms may affect the retrieved target set; thus, these results should be interpreted as exploratory. Future studies should use multiple POCD-related search terms and target databases. Finally, although STAT3 and IL6 were identified as hub genes, they were not experimentally validated in this study. Further work should examine inflammatory pathways, especially the IL6/STAT3 axis, and explore their interaction with NRF2-related antioxidant signaling in RES-mediated protection.

Acknowledgements

This study was supported by Jiangxi Province Traditional Chinese Medicine Science and-Technology Project (No. 2025021625).

Disclosure of conflict of interest

None.

Address correspondence to: Dr. Fen Liu, Department of Intensive Care Medicine, The First Affiliated

Hospital of Nanchang University, Jiangxi Provincial People's Hospital, No. 17, Yongwai Zhengjie, Donghu District, Nanchang 330006, Jiangxi, China. E-mail: ncyxy01130@163.com

References

[1] Needham MJ, Webb CE and Bryden DC. Postoperative cognitive dysfunction and dementia: what we need to know and do. Br J Anaesth 2017; 119 Suppl 1: i115-i125.

[2] Wang CM, Chen WC, Zhang Y, Lin S and He HF. Update on the mechanism and treatment of sevoflurane-induced postoperative cognitive dysfunction. Front Aging Neurosci 2021; 13: 702231.

[3] Yang X, Huang X, Li M, Jiang Y and Zhang H. Identification of individuals at risk for postoperative cognitive dysfunction (POCD). Ther Adv Neurol Disord 2022; 15: 17562864221114356.

[4] Lin X, Chen Y, Zhang P, Chen G, Zhou Y and Yu X. The potential mechanism of postoperative cognitive dysfunction in older people. Exp Gerontol 2020; 130: 110791.

[5] Li Z, Zhu Y, Kang Y, Qin S and Chai J. Neuroinflammation as the underlying mechanism of postoperative cognitive dysfunction and therapeutic strategies. Front Cell Neurosci 2022; 16: 843069.

[6] Wen J, Ding Y, Wang L and Xiao Y. Gut microbiome improves postoperative cognitive function by decreasing permeability of the blood-brain barrier in aged mice. Brain Res Bull 2020; 164: 249-256.

[7] Yang Y, Liu Y, Zhu J, Song S, Huang Y, Zhang W, Sun Y, Hao J, Yang X, Gao Q, Ma Z, Zhang J and Gu X. Neuroinflammation-mediated mitochondrial dysregulation involved in postoperative cognitive dysfunction. Free Radic Biol Med 2022; 178: 134-146.

[8] Umpierre AD and Wu LJ. How microglia sense and regulate neuronal activity. Glia 2021; 69: 1637-1653.

[9] Borst K, Dumas AA and Prinz M. Microglia: immune and non-immune functions. Immunity 2021; 54: 2194-2208.

[10] Saxena S and Maze M. Impact on the brain of the inflammatory response to surgery. Presse Med 2018; 47: e73-e81.

[11] Degos V, Vacas S, Han Z, van Rooijen N, Gressens P, Su H, Young WL and Maze M. Depletion of bone marrow-derived macrophages perturbs the innate immune response to surgery and reduces postoperative memory dysfunction. Anesthesiology 2013; 118: 527-536.

[12] Lu Z, Liu S, Lopes-Virella MF and Wang Z. LPS and palmitic acid co-upregulate microglia activation and neuroinflammatory response. Compr Psychoneuroendocrinol 2021; 6: 100048.

[13] Scordino M, Urone G, Frinchi M, Valenza C, Bonura A, Cipollina C, Ciriminna R, Meneguzzo F, Pagliaro M, Mudò G and Di Liberto V. Anti-apoptotic and anti-inflammatory properties of grapefruit IntegroPectin on human microglial HMC3 cell line. Cells 2024; 13: 355.

[14] Li Y, Ruan X, Sun M, Yuan M, Song J, Zhou Z, Li H, Ma Y, Mi W and Zhang X. Iron deposition participates in LPS-induced cognitive impairment by promoting neuroinflammation and ferroptosis in mice. Exp Neurol 2024; 379: 114862.

[15] He G, He Y, Ni H, Wang K, Zhu Y and Bao Y. Dexmedetomidine attenuates neuroinflammation and microglia activation in LPS-stimulated BV2 microglia cells through targeting circShank3/miR-140-3p/TLR4 axis. Eur J Histochem 2023; 67: 3766.

[16] Jung H, Lee D, You H, Lee M, Kim H, Cheong E and Um JW. LPS induces microglial activation and GABAergic synaptic deficits in the hippocampus accompanied by prolonged cognitive impairment. Sci Rep 2023; 13: 6547.

[17] Hoogland IC, Houbolt C, van Westerloo DJ, van Gool WA and van de Beek D. Systemic inflammation and microglial activation: systematic review of animal experiments. J Neuroinflammation 2015; 12: 114.

[18] Liao S, Wu J, Liu R, Wang S, Luo J, Yang Y, Qin Y, Li T, Zheng X, Song J, Zhao X, Xiao C, Zhang Y, Bian L, Jia P, Bai Y and Zheng X. A novel compound DBZ ameliorates neuroinflammation in LPS-stimulated microglia and ischemic stroke rats: role of Akt(Ser473)/GSK3beta(Ser9)-mediated Nrf2 activation. Redox Biol 2020; 36: 101644.

[19] Ji L, Moghal N, Zou X, Fang Y, Hu S, Wang Y and Tsao MS. The NRF2 antagonist ML385 inhibits PI3K-mTOR signaling and growth of lung squamous cell carcinoma cells. Cancer Med 2023; 12: 5688-5702.

[20] Zhou DD, Luo M, Huang SY, Saimaiti A, Shang A, Gan RY and Li HB. Effects and mechanisms of resveratrol on aging and age-related diseases. Oxid Med Cell Longev 2021; 2021: 9932218.

[21] de la Lastra CA and Villegas I. Resveratrol as an antioxidant and pro-oxidant agent: mechanisms and clinical implications. Biochem Soc Trans 2007; 35: 1156-1160.

[22] Tian B and Liu J. Resveratrol: a review of plant sources, synthesis, stability, modification and food application. J Sci Food Agric 2020; 100: 1392-1404.

[23] Hurley LL and Tizabi Y. Neuroinflammation, neurodegeneration, and depression. Neurotox Res 2013; 23: 131-144.

[24] Moussa C, Hebron M, Huang X, Ahn J, Rissman RA, Aisen PS and Turner RS. Resveratrol regulates neuro-inflammation and induces adaptive immunity in Alzheimer's disease. J Neuroinflammation 2017; 14: 1.
[25] Wei RM, Zhang YM, Feng YZ, Zhang KX, Zhang JY, Chen J, Luo BL, Li XY and Chen GH. Resveratrol ameliorates maternal separation-induced anxiety- and depression-like behaviors and reduces Sirt1-NF-kB signaling-mediated neuroinflammation. Front Behav Neurosci 2023; 17: 1172091.
[26] Guo L, Zhou Y and Ma R. Exploring the anti-gastric cancer mechanism of action of Bidentis Bipinnatae Herba based on network pharmacology, molecular docking, and cellular experimental validation. Naunyn Schmiedebergs Arch Pharmacol 2024; 397: 8681-8690.
[27] Rigden DJ and Fernández XM. The 2024 Nucleic Acids Research database issue and the online molecular biology database collection. Nucleic Acids Res 2024; 52: D1-D9.
[28] Shen KY, Dai XL, Li S, Huang F, Chen LQ, Luo P and Qu XL. Specific expression profile of follicular fluid-derived exosomal microRNAs in patients with diminished ovarian reserve. BMC Med Genomics 2023; 16: 308.
[29] Szklarczyk D, Kirsch R, Koutrouli M, Nastou K, Mehryary F, Hachilif R, Gable AL, Fang T, Doncheva NT, Pyysalo S, Bork P, Jensen LJ and von Mering C. The STRING database in 2023: protein-protein association networks and functional enrichment analyses for any sequenced genome of interest. Nucleic Acids Res 2023; 51: D638-D646.
[30] Lussi YC, Magrane M, Martin MJ and Orchard S; UniProt Consortium. Searching and navigating UniProt databases. Curr Protoc 2023; 3: e700.
[31] Kanehisa M and Sato Y. KEGG Mapper for inferring cellular functions from protein sequences. Protein Sci 2020; 29: 28-35.
[32] Shahcheraghi SH, Salemi F, Small S, Syed S, Salari F, Alam W, Cheang WS, Saso L and Khan H. Resveratrol regulates inflammation and improves oxidative stress via Nrf2 signaling pathway: therapeutic and biotechnological prospects. Phytother Res 2023; 37: 1590-1605.
[33] Tong J, Fang J, Zhu T, Xiang P, Shang J, Chen L, Zhao J, Wang Y, Tong L and Sun M. Pentagalloylglucose reduces AGE-induced inflammation by activating Nrf2/HO-1 and inhibiting the JAK2/STAT3 pathway in mesangial cells. J Pharmacol Sci 2021; 147: 305-314.
[34] Huang F, Wang X, Xiao G and Xiao J. Loganin exerts a protective effect on ischemia-reperfusion-induced acute kidney injury by regulating JAK2/STAT3 and Nrf2/HO-1 signaling pathways. Drug Dev Res 2022; 83: 150-157.
[35] Lee J, Lim JW and Kim H. Lycopene inhibits IL-6 expression by upregulating NQO1 and HO-1 via activation of Nrf2 in ethanol/lipopolysaccharide-stimulated pancreatic acinar cells. Antioxidants (Basel) 2022; 11: 519.
[36] Klotz LO, Sánchez-Ramos C, Prieto-Arroyo I, Urbánek P, Steinbrenner H and Monsalve M. Redox regulation of FoxO transcription factors. Redox Biol 2015; 6: 51-72.
[37] Yang J, Huang J, Shen C, Cheng W, Yu P, Wang L, Tang F, Guo S, Yang Q and Zhang J. Resveratrol treatment in different time-attenuated neuronal apoptosis after oxygen and glucose deprivation/reoxygenation via enhancing the activation of Nrf-2 signaling pathway in vitro. Cell Transplant 2018; 27: 1789-1797.
[38] Kesherwani V, Atif F, Yousuf S and Agrawal SK. Resveratrol protects spinal cord dorsal column from hypoxic injury by activating Nrf-2. Neuroscience 2013; 241: 80-88.
[39] Wei Y, Jia J, Jin X, Tong W and Tian H. Resveratrol ameliorates inflammatory damage and protects against osteoarthritis in a rat model of osteoarthritis. Mol Med Rep 2018; 17: 1493-1498.
[40] Zhao Q, Wan H, Pan H and Xu Y. Postoperative cognitive dysfunction-current research progress. Front Behav Neurosci 2024; 18: 1328790.
[41] Xiao MZ, Liu CX, Zhou LG, Yang Y and Wang Y. Postoperative delirium, neuroinflammation, and influencing factors of postoperative delirium: a review. Medicine (Baltimore) 2023; 102: e32991.
[42] Yuan N, Wang X, Zhang Y, Kong L, Yuan L and Ge Y. Intervention of NF-Kappab signaling pathway and preventing post-operative cognitive dysfunction as well as neuronal apoptosis. Iran J Public Health 2022; 51: 124-132.
[43] Magee JC and Grienberger C. Synaptic plasticity forms and functions. Annu Rev Neurosci 2020; 43: 95-117.
[44] Wang W, Gao W, Zhang L, Xia Z and Zhao B. SNAP25 ameliorates postoperative cognitive dysfunction by facilitating PINK1-dependent mitophagy and impeding caspase-3/GSDME-dependent pyroptosis. Exp Neurol 2023; 367: 114463.
[45] Feng X, Valdearcos M, Uchida Y, Lutrin D, Maze M and Koliwad SK. Microglia mediate postoperative hippocampal inflammation and cognitive decline in mice. JCI Insight 2017; 2: e91229.
[46] Saha S, Buttari B, Panieri E, Profumo E and Saso L. An overview of Nrf2 signaling pathway and its role in inflammation. Molecules 2020; 25: 5474.
[47] Wei YD, Chen XX, Yang LJ, Gao XR, Xia QR, Qi CC and Ge JF. Resveratrol ameliorates learning

and memory impairments induced by bilateral hippocampal injection of streptozotocin in mice. Neurochem Int 2022; 159: 105385.

[48] Rudolph JL, Schreiber KA, Culley DJ, McGlinchey RE, Crosby G, Levitsky S and Marcantonio ER. Measurement of post-operative cognitive dysfunction after cardiac surgery: a systematic review. Acta Anaesthesiol Scand 2010; 54: 663-677.

[49] Skvarc DR, Berk M, Byrne LK, Dean OM, Dodd S, Lewis M, Marriott A, Moore EM, Morris G, Page RS and Gray L. Post-operative cognitive dysfunction: an exploration of the inflammatory hypothesis and novel therapies. Neurosci Biobehav Rev 2018; 84: 116-133.